Available online at www.sciencedirect.com
SCIENCE DIRECT
Journal of Physics and Chemistry of Solids 67 (2006) 407–411
JOURNAL OF PHYSICS AND CHEMISTRY OF SOLIDS
www.elsevier.com/locate/jpcs

Charge transport in normal metal–magnesiumdiboride junctions

A. Brinkman [a,b,*], S.H.W. van der Ploeg [a], A.A. Golubov [a], H. Rogalla [a], T.H. Kim [c], J.S. Moodera [d]

[a] MESA+ Institute for Nanotechnology and Faculty of Science and Technology, University of Twente, P.O. Box 217, 7500 AE Enschede, The Netherlands
[b] DPMC, University of Geneva, Quai Ernest Ansermet 24, 1211 Genève, Switzerland
[c] Dept of Physics, Ewha Womans University, 11-1 Dae Hyun-Dong, Soe Dae Moon-Gu Seoul 120-750, Republic of Korea
[d] Francis Bitter Magnet Lab, Massachusetts Institute of Technology, 170 Albany Street, Cambridge, Massachusetts 02139, USA

Abstract

The influence of the multiband nature of superconductivity in MgB_2 on the charge transport properties of MgB_2 tunnel junctions and normal metal–MgB_2 heterostructures has been theoretically modeled and experimentally explored. The conductance as function of barrier height and angle is calculated. Planar *c*-axis tunnel junctions are realized in which two gaps are resolved in the tunnel spectrum. For junctions with additional conductance in the direction of the crystallographic *a–b* plane we observe a sharp resonance that can possibly be attributed to a Leggett mode.

1. Introduction

MgB_2 is a prototype multiband superconductor [1] and the material is therefore a playground for investigating novel physical phenomena related to multiband conductivity, such as the co-existence of multiple superconducting gaps, interband interactions, and phase oscillations between the superconducting condensates.

On top of the interest in the fundamental physics of multiband effects, MgB_2 is promising for electronic applications because of its relatively large superconducting transition temperature of 39 K and its metallic character. In order to fully benefit from the superconducting properties of MgB_2, Josephson devices are desired with transport in the crystallographic *a–b* plane [2]. Therefore, it is necessary to understand the conductance of MgB_2 heterostructures as function of barrier and angle.

Point-contact spectroscopy and scanning tunneling microscopy have revealed already important properties of MgB_2 [1,3]. The next challenging step would be to model, realize and investigate epitaxial tunnel junctions. First attempts to achieve multilayer *c*-axis tunnel junctions are being reported [4–7] as well as *a–b* plane multilayer junctions [8,9].

Here, we focus on the observation and modelling of charge transport properties in heterostructures that contain MgB_2. A theoretical tunneling model is derived from which the conductance of normal metal–tunnel barrier–MgB_2 structures can be calculated as function of barrier height and angle, taking the specific Fermi-surface topology into account. MgB_2 heterostructures that allow to do tunnel spectroscopy are experimentally realized. The two gaps in MgB_2 are resolved and a resonance is observed that can possibly be attributed to a collective excitation corresponding to fluctuations of the relative phase of the two condensates as predicted by Leggett [10].

2. Charge transport in heterostructures

2.1. Proximity effect

The proximity effect is the phenomenon that a superconducting order parameter can penetrate from a superconductor (S) into a normal metal (N), or another superconductor (S′) with a critical temperature $T_{cS'} < T_{cS}$, over a distance of the order of the coherence length, inducing a minigap in N or S. This phenomenon is well understood, both in terms of Andreev reflections as well as in terms of microscopic Green's functions.

The manifestation of the proximity effect in MgB_2 was recently modeled in Ref. [11] on the basis of the Usadel Green's functions approach. For this purpose, multiband boundary conditions for the quasi-classical Green's functions were derived. On top of the existing interband coupling in MgB_2, the boundary conditions at a normal metal–MgB_2 interface form an additional coupling between the bands. It is

* Corresponding author
E-mail address: a.brinkman@tnw.utwente.nl (A. Brinkman).

0022-3697/$ - see front matter © 2005 Elsevier Ltd. All rights reserved.
doi:10.1016/j.jpcs.2005.10.013

predicted [11] that superconductivity can even be enhanced by the proximity to a superconductor with a lower T_c.

In the following, we will assume the pair potentials in MgB_2 to be constant towards the interface. The proximity effect than solely appears as a non-vanishing coefficient for Andreev reflection. This approximation is valid as long as an interface barrier is present which can already be provided by a mismatch in the Fermi-velocities at the interface.

2.2. Normal metal–superconductor conductance

Tunneling effects in MgB_2 have already been theoretically modeled on the basis of the Eliashberg formalism using first principles calculation results [2]. The Josephson and quasi-particle tunnel characteristics were obtained based on the approximation that the ratio of the tunnel conductances of different bands is given by the square of the ratio of the respective plasma frequencies. Here, we go beyond this approximation and take the specific MgB_2 Fermi-surface topology into account.

The model of Blonder et al. [12] describes all scattering probabilities at a one-dimensional contact between two free electron gases. The model can be extended to take into account a Fermi-velocity mismatch and the three-dimensional nature of the contact (see also Refs. [13,14]).

We can write the current as the following integral

$$I_{\mathrm{NIS}} = \frac{2e\mathcal{A}\Delta}{\hbar(2\pi)^3}\int \hat{\mathbf{v}}_N \cdot \hat{\mathbf{e}}_x T(\tilde{E}, v_{n,N}, v_{n,S}) \times \left[f_0(E-eV) - f_0(E)\right] \mathrm{d}\tilde{E}\, \mathrm{d}^2 S_F, \quad (1)$$

where $\mathcal{A}$ is the junction area, $\hat{\mathbf{v}}_N$ the Fermi velocity on the N side, $v_{n,N(S)}$ are the Fermi-velocity components in the direction normal ($\hat{\mathbf{e}}_x$) to the interface at the $N(S)$ side, and $f_0(E) = [\exp(E/k_B T)+1]^{-1}$ is the Fermi distribution function. The transfer function T can be expressed as

$$T(\tilde{E}) = \begin{cases} \dfrac{2}{\tilde{E}^2 + |\tilde{\xi}_k|^2 \zeta^2} & \text{for } |\tilde{E}| < 1, \\ \dfrac{2|\tilde{E}|}{|\tilde{E}| + \tilde{\xi}_k \zeta} & \text{for } |\tilde{E}| > 1, \end{cases} \quad (2)$$

where $\tilde{E} = E/\Delta$ and $\tilde{\xi}_k = \xi_k/\Delta = \sqrt{\tilde{E}^2 - 1}$ are the normalized total and kinetic energy of the superconductive quasi-particles. The dimensionless parameter ζ is a function of the same parameters as the normal state transfer function given by

$$\zeta = \frac{4W^2 + v_{n,N}^2 + v_{n,S}^2}{2 v_{n,N} v_{n,S}}, \quad (3)$$

where W is the specular barrier height. The direction and magnitude of the Fermi velocity are given by electronic structure calculations. The direction of the Fermi velocity is normal to the Fermi surface while the magnitude is determined by the effective mass.

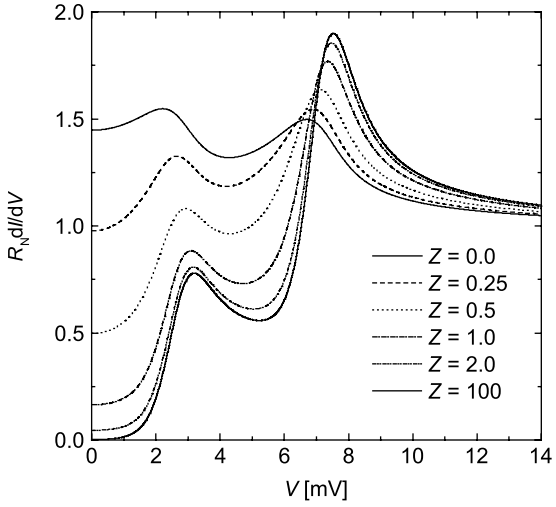

Fig. 1. Normalized conductance of a N–I–MgB_2 heterostructure for transport in the crystallographic a–b plane direction, at $T=0$. The parameter Z is varied from $Z=0$ (Andreev contact) to $Z \gg 1$ (tunneling). The values for Δ_π and Δ_π are taken from Ref. [2].

For MgB_2 we use the simplified band structure as introduced by Dahm and Schopol [15]. In this model the quasi two-dimensional σ-band is described by a distorted cylinder. We shifted the half torus, which is used to model the π-band, along the LM line, to correspond better to the full Fermi-surface as calculated by Kortus et al. [16].

We calculate the current into each band separately and consequently sum the contributions. This implies some approximation for the case in which both bands overlap, since we then allow for the possibility of a single electron tunneling into more than one band. However, the Fermi-area for which this is the case is quite small for tunneling along the a–b plane and entirely absent in the case of c-axis tunneling. Additionally, in the high-barrier limit $T \ll 1$, hence, only a small overestimate of the current in the low-barrier limit exists. In first approximation the ratio between the currents is not affected and neither is the normalized conductivity.

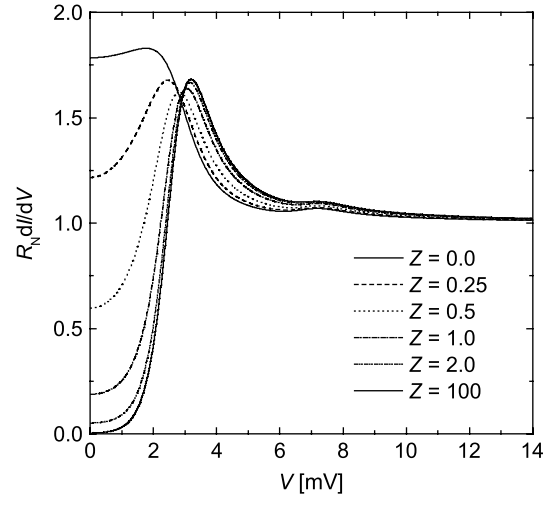

Fig. 2. Normalized conductance of a N–I–MgB_2 heterostructure for transport in the crystallographic c-axis direction.

As an example, we consider the case of an Au normal metal counter electrode. Figs. 1 and 2 show the results of a numerical integration of Eq. (1) for transport in the *c*-axis and *a–b* plane directions respectively. The conductance is calculated as function of the barrier parameter $Z = W/v_{F,N}$, ranging from Andreev conductance ($Z=0$) to tunneling ($Z \gg 1$).

The double-gap feature is especially pronounced when transport occurs along the *a–b* plane. In the case of *c*-axis transport, the contribution of the σ-band to the conductivity is small, albeit slightly larger than was estimated from a simple argument in terms of the plasma frequencies [2].

Note, that for $Z=0$, no doubling of the zero-bias conductance is obtained, due to the mismatch of the Fermi-velocities at the two sides of the interface which make the barrier effectively less transparent. This effect is especially pronounced in the *a–b* plane direction.

3. Experimental observations

3.1. Device realization

MgB_2 thin films were grown by Molecular Beam Epitaxy, using two separate sources for magnesium and boron, see Ref. [17] for details. The *c*-axis oriented films are grown on Si(111), using an MgO bufferlayer.

Planar MgB_2–Al_2O_3–Al heterostructures were grown in situ, the Al being the normal metal counter electrode in this case. The Al_2O_3 barrier layer was realized by a deposition of Al followed by active oxidation in an ozone atmosphere. The multilayers were consequently structured by making use of the ramp-type junction configuration to make contacts to the bottom and counter electrodes. The Al counter electrode is connected to a dc sputter deposited Al wiring layer after etch-cleaning the interface. Insulation between bottom and counter electrode is provided by RF sputter deposited SiO_2. The resulting structure after all fabrication steps is schematically depicted in the inset of Fig. 3.

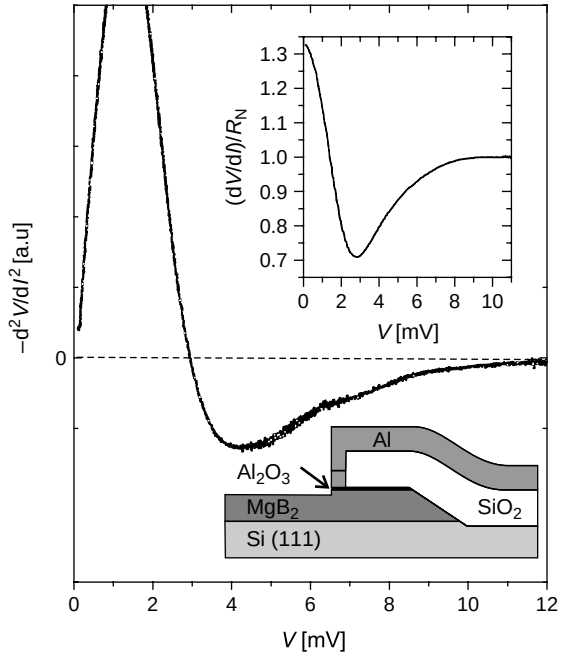

Fig. 3. Second derivative tunnel spectrum of a *c*-axis Al–Al_2O_3–**MgB_2** contact, of which the d*V*/d*I* tunnel spectrum is shown in the inset, as well as the layout of the heterostructure.

3.2. C-axis tunnel junctions

We measured the current–voltage characteristics of the planar tunnel junctions in a shielded variable temperature cryostat from 4 K to well above the transition temperature of the MgB_2 (about 30 K for these junctions). The first derivative dV/dI and second derivative d^2V/dI^2 were measured, respectively, with the first and second harmonic signal of a lock-in amplifier when the sample was additionally biased with a few μA ac current.

The normal state conductance of most *c*-axis junctions roughly scaled with the junction area (overlap of the ramp and bottom electrode times junction width). A typical example of a measured second derivative d^2V/dI^2 tunnel spectrum is shown in Fig. 3. The steep zero-crossing around 2.5 mV can be attributed to Δ_π while the small hump around 6.5 mV corresponds to the small conductance contribution of the σ-band. The dV/dI spectrum is shown in the inset of Fig. 3. By comparing the dV/dI spectrum with the theoretically expected spectra of Fig. 2, one can see that the obtained barrier parameter Z is not yet the ideal tunnel value (much larger than one), probably due to shunts in the barrier. The spectrum can be fitted with the model as described above, the magnitude of the σ-band conductance being a few percent.

3.3. Possible observation Leggett mode

Incidentally, in one set of *c*-axis tunnel junctions, the SiO_2 insulator layer contained oxygen vacancies, which can typically give rise to a conducting surface layer. It can be seen in the inset of Fig. 3 that this layer could lead to a conductance shunt in the direction of the ramp, resulting in an *a–b* plane conductance component. The SiO_2 surface layer resistance could not be measured directly due to the layer's specific location in the ramp structure. The shunt can be modeled within our formalism by adding a low-Z *a–b* plane conductance to a *c*-axis tunnel conductance. The example for a shunt with $Z=0$ is shown in Fig. 4 for two different temperatures. The qualitative difference between the two curves is caused by the dependence of the gaps on temperature.

The measured dV/dI spectrum of a shunted junction is shown in Fig. 5 as function of temperature. The overall conductance of the spectra corresponds to the theoretical expectation of the additional *a–b* plane conductance shunt, but other types of shunts should not be excluded. The energy scales of both gaps are clearly resolved: the *c*-axis tunneling contribution appears as the expected conductance drop below Δ_π/e(=2.5 mV at 4 K), while the *a–b* plane contribution also contains a conductance increase at $V=6$–8 mV.

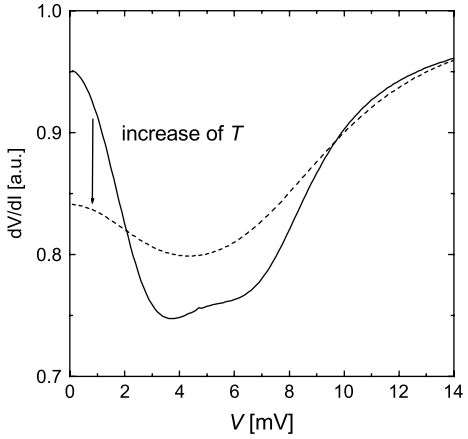

Fig. 4. Model result for the conductance of a *c*-axis tunneling channel parallel to a *a*–*b* plane $Z=0$ conductance channel, in the case of an N–I–MgB_2 heterostructure at 10 K (solid line) and 20 K (dashed line). The full Fermi-surface was taken into account, where the N metal was chosen to be Au.

Very striking is the sharp resonance in the spectra of these junctions, which was measured to be independent from the measurement procedure or the electronics used. The resonance appears at a voltage between Δ_π/e and Δ_σ/e and roughly has the same temperature dependence as Δ_σ/e. The resonance can be resolved in the spectra up to the superconducting transition temperature.

The resonance could be a manifestation of a collective excitation of the relative phase of the σ and π condensates. This mode was predicted for multiband superconductors in 1966 by Leggett [5]. For MgB_2, the Leggett mode is expected [18] to appear at energy E_{res} for which

$$E_{\mathrm{res}}^2 = 4\Delta_\pi\Delta_\sigma \frac{\lambda_{\sigma\pi}+\lambda_{\pi\sigma}}{\lambda_{\sigma\sigma}\lambda_{\pi\pi}-\lambda_{\sigma\pi}\lambda_{\pi\sigma}}, \tag{4}$$

where λ_{ij} are the coupling constants. Using the coupling constants and energy gaps from band structure calculations [2], it is found at $T=0$ that $E_{\mathrm{res}}=8$ meV, which is close to the value that we observe, taken the reduction of the T_c of our films into account. Since the mode occurs at an energy larger than twice the smaller gap, the mode is expected to be broadened.

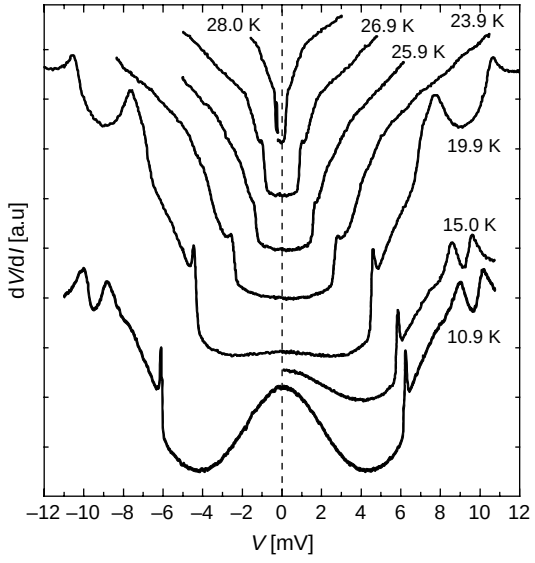

Fig. 5. *d*V/*d*I tunnel spectra in which the sharp resonance can possibly be identified as a Leggett mode. The curves have been shifted vertically for clarity.

4. Conclusion

We have modeled the conductance of multilayered normal metal–MgB_2 contacts in the range from tunnel junctions to Andreev contacts. The model allows to calculate the conductance for arbitrary angle and can easily be extended to take into account the thickness of the barrier.

The two gaps of MgB_2 were observed in the tunnel spectrum of a *c*-axis oriented MgB_2–Al_2O_3–Al junction. Junctions with a possible additional conductance along the *a*–*b* plane direction showed a sharp resonance in the conductance spectrum. The resonance voltage scales with Δ_σ and could possibly be interpreted as a Leggett resonance.

In Ref. [19], an optical plasmon mode was observed in the optical spectrum of $SmLa_{0.8}Sr_{0.2}CuO_{4-\delta}$ and interpreted in terms of Leggett's predicted collective excitation. The question why a Leggett mode could be excited under dc current bias as we possibly observed (the ac frequency used for the lock-in amplifier being much lower than the typical ac Josephson frequency) has theoretically not yet been resolved. Several MgB_2 tunnel junctions have been realized in which no Leggett mode was observed [4–7]. The data from Refs. [20] and [21] also hint at a collective excitation influencing the transport properties. However, in our experiment, Josephson effects between the counter electrode and MgB_2 can be excluded, as well as a sub-harmonic gap structure due to multiple Andreev reflections. A clue to our observations might be the fact that we have only measured the resonance in junctions with a considerable shunt, possibly in the crystallographic *a*–*b* plane direction, which had not been realized in tunnel junctions before.

Acknowledgements

We gratefully acknowledge useful discussions with O.V. Dolgov, H. Hilgenkamp, M.Yu. Kupriyanov, D. van der Marel, and I. Mazin. This work is supported by the Netherlands Organization for Scientific Research (NWO) and the Dutch Foundation for Research on Maffer (FOM).

References

[1] Physica C 385 (1–2) (2003) (Special issue on MgB_2).
[2] A. Brinkman, A.A. Golubov, H. Rogalla, O.V. Dolgov, J. Kortus, Y. Kong, O. Jepsen, K. Andersen, Phys. Rev. B 65 (2002) 180517.
[3] I.K. Yanson, Y.G. Naidyuk, Low Temp. Phys. 30 (2004) 261.
[4] A. Saito, A. Kawakami, H. Shimakage, H. Terai, Z. Wang, IEEE Trans. Appl. Supercond. 13 (2003) 1067.
[5] K. Ueda, M. Naito, IEEE Trans. Appl. Supercond. 13 (2003) 3249.
[6] T.H. Kim, J.S. Moodera, Appl. Phys. Lett. 85 (2004) 434.
[7] G. Carapella, N. Martuciello, G. Costabile, C. Ferdeghini, V. Ferrando, G. Grassano, Appl. Phys. Lett. 80 (2002) 2949.

[8] D. Mijatovic, A. Brinkman, I. Oomen, G. Rijnders, H. Hilgenkamp, H. Rogalla, D.H.A. Blank, Appl. Phys. Lett. 80 (2002) 2141.
[9] J.I. Kye, H.N. Lee, J.D. Park, S.H. Moon, B. Oh, IEEE Trans. Appl. Supercond. 13 (2003) 1075.
[10] A.J. Leggett, Progr. Theor. Phys. 36 (1966) 901.
[11] A. Brinkman, A.A. Golubov, M.Yu. Kupriyanov, Phys. Rev. B 69 (2004) 214407.
[12] G. Blonder, M. Tinkham, T. Klapwijk, Phys. Rev. B 25 (1982) 4515.
[13] N.A. Mortensen, K. Flensberg, P. Jauho, Phys. Rev. B 59 (1999) 10176.
[14] M. Kupka, Physica C 281 (1997) 91.
[15] T. Dahm, N. Schopol, Phys. Rev. Lett. 91 (2003) 17001.
[16] J. Kortus, I.I. Mazin, K.D. Belashchenko, V.P. Antropov, L.L. Boyer, Phys. Rev. Lett. 86 (2001) 4656.
[17] A.J.M. van Erven, T.H. Kim, M. Muenzenberg, J.S. Moodera, Appl. Phys. Lett. 81 (2002) 4982.
[18] S.C. Sharapov, V.P. Gusynin, H. Beck, Eur. Phys. J. B30 (2002) 45.
[19] D. Dulić, et al., Phys. Rev. Lett. 86 (2001) 4144.
[20] Ya.G. Ponomarev, et al., Solid State Commun. 129 (2004) 85.
[21] Ya.G. Ponomarev, et al., Pis'ma ZhETF 79 (2004) 597.